Clays and Clay Minerals, Vol. 40, No. 5, 575–585, 1992.

DITHIONITE AS A DISSOLVING REAGENT FOR GOETHITE IN THE PRESENCE OF EDTA AND CITRATE. APPLICATION TO SOIL ANALYSIS

ELSA H. RUEDA, MARÍA C. BALLESTEROS, AND REYNALDO L. GRASSI
Departamento de Química e Ingeniería Química, Universidad Nacional del Sur
Avenida Alem 1253, (8000) Bahía Blanca, Argentina

MIGUEL A. BLESA
Departamento Química de Reactores, Comisión Nacional de Energía Atómica
Avenida del Libertador 8250, (1429) Buenos Aires, Argentina

Abstract—A synergistic effect of reductant and complexant is observed in the dissolution of goethite by dithionite and citrate or EDTA. The rate data are interpreted using the surface complexation approach to describe the interface of the reacting oxide. Adsorption of both $S_2O_4^{2-}$ (D) and complexant (L) generates three surface complexes that define the dissolution behavior: ≡Fe-D, ≡Fe-L, and dimeric $\left|\begin{matrix}\equiv\text{Fe D}\\ \equiv\text{Fe L}\end{matrix}\right.$ surface complexes. The initial rate increases at lower pH values because of increased surface complexation conditional formation constants. At pH values below 4, however, the fast decomposition of $S_2O_4^{2-}$ gives rise to a rapid depletion of reductant, and total dissolution is not observed. It is shown that for best analytical results in soil analysis, EDTA is a better complexant than citrate; the iron extracted in one dithionite-EDTA treatment at pH 5–6, under N_2 at 315 K is not increased by increasing the number of extractions, and is equivalent to the total extractable iron found by previous procedures.

Key Words—Dithionite, Goethite, Iron analysis, Iron dissolution.

INTRODUCTION

Because of the limited stability of $Fe(OH)_3(aq)$, the dissolution of iron oxides requires the consumption of either H^+ or OH^- to generate ionic species such as $Fe(H_2O)_6^{3+}$, $Fe(H_2O)_6^{2+}$ or $Fe(OH)_4^-$. The acid dissolution is by far more important, and solutions aggressive to iron oxides usually contain large acid capacities, either in the form of high H^+ concentrations, or in the form of weak acids that are good iron(III) complexants (EDTA anions constitute a typical example). Most of the studies on the mechanism of dissolution of iron oxides have therefore dealt with fairly acidic solvents (Blesa *et al.*, 1988). Paradoxically, neutral or even alkaline media in practice are more important in many cases: mobilization of iron in the ground and in biological media are two examples. The search for alkaline or neutral solvents also constitutes an important chapter in the history of chemical cleaning of metal surfaces, achieving very limited success through the use of hydrazine and/or EDTA (or similar carboxylic acids).

The only reagents known to be effective at pH > 5 were developed for soil analysis: dithionite (Deb, 1950; Aguilera and Jackson, 1953; Mehra and Jackson, 1960), and Ti(III) in the presence of citrate and EDTA (Ryan and Gschwend, 1991). Both reagents dissolve iron(III) reductively, and constitute examples of two large classes of reductants: complexing anions, and low oxidation metal complexes (Blesa *et al.*, 1992a). Briefly, these reagents are known to form inner sphere complexes with surface iron(III) ions that later evolve through charge transfer from the reductant complexing anion or from the bridged reduced metal ion (Blesa *et al.*, 1992a, 1992b).

As early as 1950 Deb proposed $S_2O_4^{2-}$/tartrate or $S_2O_4^{2-}$/acetate at pH 5–6 for iron analysis in soils, which procedure was later modified by Aguilera and Jackson (1953) and by Mehra and Jackson (1960). The final result was the classical procedure to assay crystalline iron oxides in soils. Dithionite/citrate became a model solvent; it was used by Torrent *et al.* (1987) to probe the changes in reactivity in iron oxides brought about by adsorption, ionic substitution, or other factors. The objective of this paper is to derive the mechanism of the dissolution process. The study of the kinetics of dissolution of goethite by dithionite/EDTA and dithionite/citrate also permits the optimization of the composition of the solvent to be used in soil analysis, and a better recognition of the limitations of the reagent.

EXPERIMENTAL METHODS

Goethite was prepared as described by Atkinson *et al.* (1968) and by Rochester and Topham (1979): 15 ml NaOH 2.5 mol dm^{-3} were added to 85 ml of water

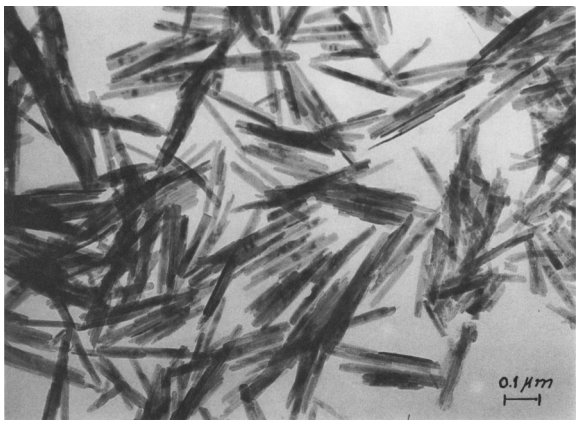

Figure 1. Transmission electron micrograph of goethite particles.

containing 0.05 moles $Fe(NO_3)_2 \cdot 9H_2O$, yielding a solution of pH 1.6. This solution was aged at 298 K for 50 h and later poured over 100 ml NaOH 2.5 mol dm^{-3}. The resulting suspension was aged at 336 K for 3 days, and the solid was collected by decantation, filtration, and repeated rinsing. Electron microscopy showed it to be composed of acicular particles, modal length 0.3 μm, and modal diameter of about 30 nm. No impurities were apparent from powder X-ray diffraction patterns. BET specific surface area was measured to be 68 $m^2\ g^{-1}$ in a Micromeritics Accusorb apparatus. Oxalate extraction (Mc Keague and Day, 1966) showed the presence of <0.6% amorphous oxide. Potentiometric titrations yielded a point of zero charge (pH_0) of 8.65 (Rueda, 1988), in good agreement with other literature values (Hingston *et al.*, 1972; James *et al.*, 1975; Bowden *et al.*, 1980). All reagents were analytical grade and water was bi-distilled.

Kinetic experiments were performed in a sealed cylindrical beaker provided with a thermostat water jacket. Solutions of citrate or EDTA of suitable pH and concentration were carefully de-aerated by bubbling nitrogen (previously scrubbed through a pyrogallol and water trap) for 30 min. Next, the desired amount of solid sodium dithionite was added and the dissolution was started by pouring goethite into the solution. After the addition of each solid, the vessel was stoppered again and N_2 bubbling restored. The solution was magnetically stirred throughout the experiment.

The dissolution reaction was followed by measuring the amount of iron released at regular time intervals. Samples were withdrawn from the suspension with a syringe and filtered through a Nuclepore membrane (pore size 0.22 μm). Iron was determined colorimetrically with thiocyanate (Hsu, 1967) with some modifications to avoid EDTA interference (citrate does not interfere): 7 ml HNO_3 mol dm^{-3} were used in 50 ml solution, instead of 3 ml as proposed by Hsu (1967).

To check the possible contribution of small particles to our measured 'dissolved iron,' some experiments were ended by quenching the reaction with alkaline thioglycollate (Baumgartner *et al.*, 1983), filtering off the solid, and measuring the absorptivity of $Fe(OH)(SCH_2CO_2)_2^{2-}_2$ at 530 nm. Any possible residual solid does not contribute to the absorptivity. Both procedures yielded identical results.

In the course of dissolution, pH changes because dissolution itself consumes H^+, whereas $S_2O_4^{2-}$ decomposition releases H^+; at pH $\lesssim$ 5, the former effect dominates whereas at pH $\gtrsim$ 5, the second one is most important. In our experiments acid or base was added as required to maintain constant pH. Only a few experiments were performed at pH > pH_0. As expected, the rates of dissolution were low.

Experiments were carried out under subdued laboratory light. No evidence of photo-assisted dissolution was found, as expected for reactions with no noticeable induction period (Litter *et al.*, 1991).

Most of the experiments were carried out at 315 K. At this temperature, the reaction proceeds at adequate rates. For the determination of the activation energy of the reaction, additional experiments in the temperature range 303 to 353 K were performed. Increasing temperature increases not only the rate of dissolution, but also the rate of dithionite decomposition. This is probably one of the reasons why several additions of dithionite are required in the procedure of Mehra and Jackson (1960) at 353 K (see below).

RESULTS

Goethite particles show the expected typical acicular habit, the long axis being perpendicular to (001) planes (Figure 1). Cornell *et al.* (1974) showed that preferential attack takes place on (001) and (010) faces, while dissolution of (100) faces is slower. Similar conclusions were suggested by our direct TEM observations.

Figure 2 shows the dissolution behavior of goethite up to large dissolution fractions. The fraction of dissolved solid $f \equiv (w_0 - w)/w_0$, where w is the mass of undissolved solid and w_0 the initial mass, is plotted as a function of time. The shape of the f/t profile can be accounted for by either three- or two-dimensional contracting geometry kinetic laws (Brown *et al.*, 1980). The latter case is more suitable to describe goethite dissolution because of the noted lower reactivity of (001) faces. The contracting geometry rate law (1) results when the specific rate (per unit surface area) is constant and the surface area decreases as expected from simple geometric considerations if only (010) and (100) faces are reactive:

$$1 - (1 - f)^{1/2} = k't. \qquad (1)$$

For k' to be constant throughout an experiment, it is required that all relevant solution variables remain constant. The fast decomposition of $S_2O_4^{2-}$, especially in more acidic media, and complications associated

https://doi.org/10.1346/CCMN.1992.0400512 Published online by Cambridge University Press

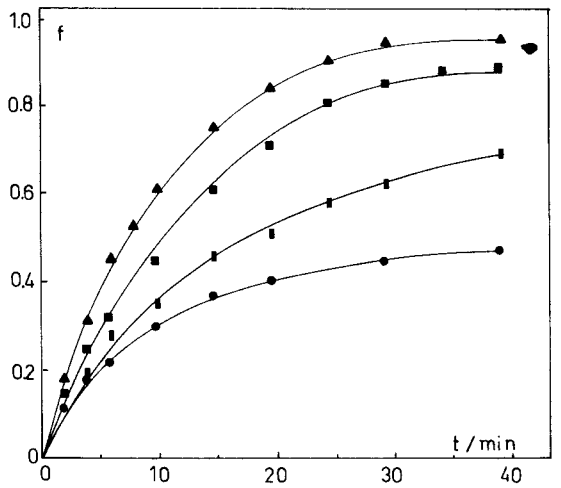

Figure 2. Fraction of total iron released from goethite as a function of time; pH 7.3, T = 315 K; goethite load 0.22 g dm^{-3}; [citrate] 0.3 mol dm^{-3}. Lines were drawn only as a visual aid. $[S_2O_4^{2-}] \times 10^{-3}$ (mol dm^{-3}) as follows: (●) 3.85; (■) 5.11; (■) 7.67; (▲) 12.77.

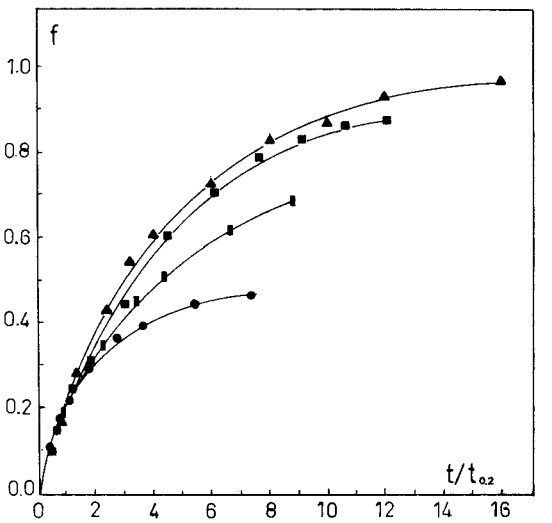

Figure 3. Affine transformation of Figure 2. Each curve is shifted horizontally by dividing the time by $t_{0.2}$, the time required to achieve f = 0.2. Lines were drawn only as a visual aid.

with the influence of dissolved Fe(II) limit the validity of Eq. (1). These deviations are clearly seen in Figure 3, where f is plotted as a function of $t/t_{0.2}$ ($t_{0.2}$ is the time required to achieve 20% dissolution) for a series of experiments of different dithionite concentrations. Absolute validity of Eq. (1) should lead to a single master curve embodying all data points (Gorichev and Kipriyanov, 1981). There is a good overlap only at low conversions, but departures are important for $f > 0.25$, especially at low dithionite concentrations. Figure 3 reflects essentially the complications associated with $S_2O_4^{2-}$ depletion by dissolution and, more importantly, by decomposition. The complications due to the build-up of Fe(II) are not evident from our data; for example, there is no indication of sigmoidal f/t profiles as found in other systems (Borghi *et al.*, 1991, dos Santos Afonso *et al.*, 1990; Blesa *et al.*, 1987). However, a small acceleration due to Fe(II) is always possible, especially at low pH values, and would result in an overestimation of k′ (Blesa *et al.*, 1992a). We have therefore chosen to discuss the kinetics of the process in terms of the initial rates (R), measured as the slope of the f/t plots at t = 0. It may be easily shown that, for bi-dimensional contracting geometry, R is related to k′ through Eq. (2):

$$R = \left\{\frac{df}{dt}\right\}_{t=0} = 2k' \qquad (2)$$

All reported R data are initial slopes, obtained graphically from plots like Figure 2. They are subjected to errors that depend essentially on the absolute values of the initial rates, i.e., on the f values at the time of the first sampling. These values are typically in the range $f < 0.2$. Extrapolation of the curve drawn through points at longer reaction times, down to t = 0, was always used as an auxiliary tool to better define the initial slopes. This procedure was chosen because it is believed to be the safest one, although it precludes an objectively accurate determination of the errors that affect R values. These errors are more important in the case of very fast reactions.

The dependence of R on the concentration of EDTA and citrate, [L], at constant $[S_2O_4^{2-}]$ and pH, at 315 K, is shown in Figures 4 and 5. The advantage of using added complexing agent is clear, but it is also shown that, from the point of view of rate alone, excessive amounts of complexants are not beneficial. The curves show that $S_2O_4^{2-}$ alone is able to dissolve goethite, but this system is further complicated by the occurrence of iron reprecipitation in all cases in which $S_2O_4^{2-}$ does not suffice to dissolve all the oxide. The $[Fe]_{diss}/t$ profiles (not shown) pass through a maximum (Rueda, 1988) and the TEM observations demonstrate the formation of a new phase. Magnetite formation by reaction of aqueous Fe(II) and Fe(III) oxides is well documented (Regazzoni *et al.*, 1981; Ardizzone and Formaro, 1983; Tamaura *et al.*, 1983; Tronc *et al.*, 1982).

The influence of dithionite concentration [D] at constant [L] and pH, at 315 K, is shown in Figure 6. The experimental points are shown together with the model curves to be discussed below; we attribute the apparent near constancy of the rate data in EDTA at high $S_2O_4^{2-}$ concentrations to the large experimental errors associated with the measurement of initial slopes in very fast reactions. The concentrations of EDTA and citrate were chosen in the region of the plateaus of Figures 4 and 5, i.e., at rather high values of [L]. Ideally,

https://doi.org/10.1346/CCMN.1992.0400512 Published online by Cambridge University Press

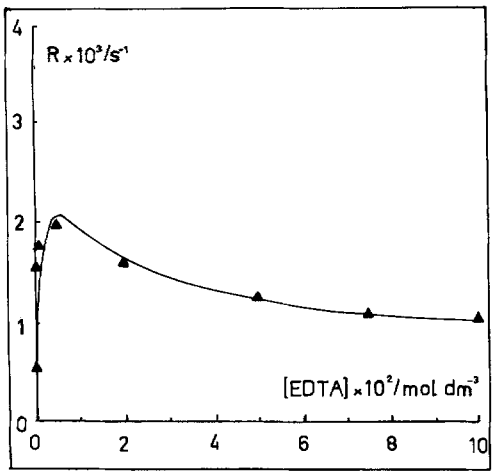

Figure 4. Initial dissolution rates R as a function of $[EDTA]_0$; pH 7.3; T = 315 K; $[S_2O_4^{2-}]_0 = 2.55 \times 10^{-3}$ mol dm^{-3}; goethite 0.22 g dm^{-3}; (▲) experimental; (——) calculated through Eq. (15) using parameter values given in Table 1.

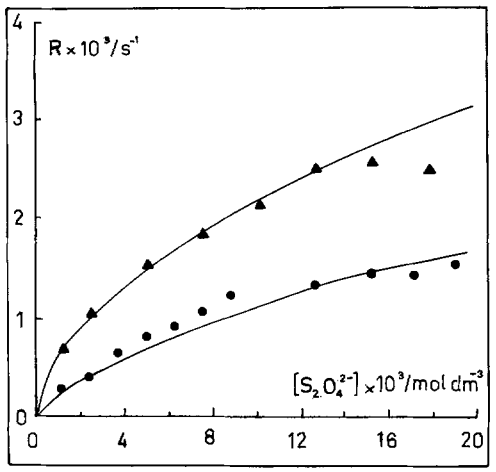

Figure 6. Initial dissolution rates R as a function of $[S_2O_4^{2-}]_0$; pH 7.3; T = 315 K. (▲): $[EDTA]_0 = 0.1$ mol dm^{-3}; goethite 0.22 g dm^{-3}. (●): $[citrate]_0 = 0.3$ mol dm^{-3}; (——) calculated through Eq. (15) using parameter values given in Table 1.

additional experiments should have been performed at lower L concentrations, but the sensitivity of the rate to [L] in these conditions makes these experiments more difficult. The information collected by us suffices to derive the mechanism discussed below.

The influence of pH on R is shown in Figure 7, which includes experimental points and curves drawn assuming a partial kinetic order on H^+ is 0.5 for EDTA and 0.6 for citrate based solvents, as discussed below.

The temperature dependence in citrate medium is shown in the Arrhenius plot of Figure 8, yielding an apparent activation energy of 70 kJ mol^{-1}. In this series of experiments, a lower EDTA concentration was used to avoid the precipitation of the free acid at low pH values.

The extraction of Fe from an Entisol soil from Médanos (Buenos Aires Province) was used to check the procedure. The traditional Mehra and Jackson analysis yielded the value 0.576% after four dithionite additions. The results of several experiments under the modified conditions are shown in Figure 9. The main conclusions are that (a) the total extractable Fe is higher (0.66%) than the value obtained by the traditional Mehra and Jackson procedure; (b) at pH 5 and 5.5 the

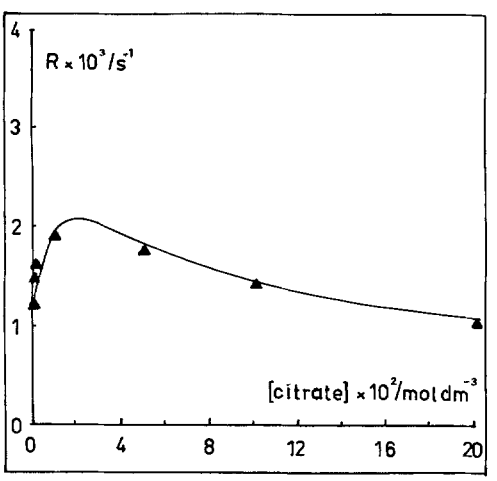

Figure 5. Initial dissolution rates R as a function of $[citrate]_0$; pH 7.3; T = 315 K; $[S_2O_4^{2-}]_0 = 7.67 \times 10^{-3}$; goethite 0.22 g dm^{-3}. (▲) experimental; (——) calculated through Eq. (15) using parameter values given in Table 1.

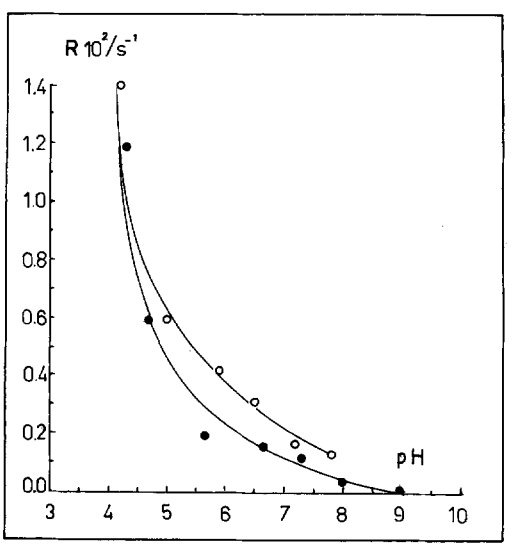

Figure 7. Initial dissolution rates R as a function of pH; T = 315 K; goethite 0.22 g dm^{-3}. (●) $[citrate]_0 = 0.3$ mol dm^{-3}; $[S_2O_4^{2-}]_0 = 7.67 \times 10^{-3}$ mol dm^{-3}. (○) $[EDTA]_0 = 0.01$ mol dm^{-3}; $[S_2O_4^{2-}]_0 = 2.55 \times 10^{-3}$ mol dm^{-3}.

https://doi.org/10.1346/CCMN.1992.0400512 Published online by Cambridge University Press

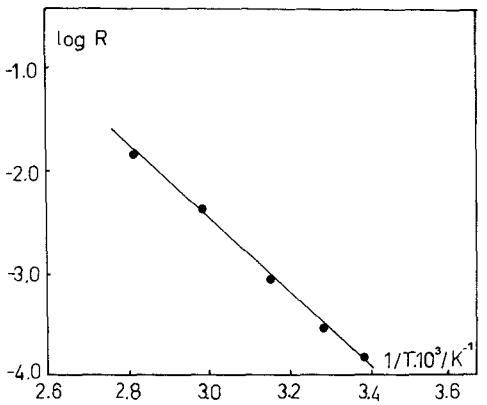

Figure 8. Arrhenius plot for the initial dissolution rates. $[S_2O_4^{2-}]_0 = 7.67 \times 10^{-3}$ mol dm^{-3}; $[citrate]_0 = 0.3$ mol dm^{-3}; goethite 0.22 g dm^{-3}; pH 7.3.

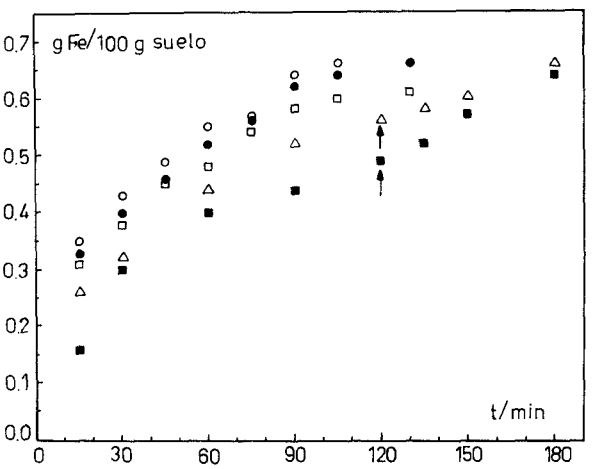

Figure 9. Time evolution of the iron extracted from an Entisol soil by the modified procedure proposed in this paper; arrows indicate a second dithionite addition. $[S_2O_4^{2-}]_0 = 6.38 \times 10^{-2}$ mol dm^{-3}; T = 315 K; (○): [EDTA] = 5×10^{-2} mol dm^{-3}, pH 5; (●) [EDTA] = 5×10^{-2} mol dm^{-3}, pH 5.5; (□) [EDTA] = 5×10^{-2} mol dm^{-3}; pH 6.0; (■) [EDTA] = 5×10^{-2} mol dm^{-3}, pH 7.0; (△) [citrate] = 0.145 mol dm^{-3}, pH 5.5.

maximum value is attained in one application of 130 min. Further additions of $S_2O_4^{2-}$ do not dissolve more iron; (c) at pH > 6, more than one $S_2O_4^{2-}$ addition are required to extract all Fe; (d) at pH 5 and 5.5, the pH does not change, and acid or base additions are not needed; (e) temperatures higher than 42°C are not required: exploratory experiments showed increased dithionite decomposition, without further Fe extraction.

The selectivity of the procedure has not been assessed yet; further work is planned to explore the behavior of aluminum and silicon, and to test other soils.

DISCUSSION

The morphology of the attack

Although our evidence does not warrant a detailed analysis of the morphology of the attack, the results of Cornell *et al.* (1976) must be taken into account in the modelling of dissolution according to the surface complexation approach.

The preferential attack on facets (001) and (010) in the dissolution of goethite by mineral acids (Cornell *et al.*, 1976) is determined by the properties of the coordination polyhedra of exposed Fe ions in each type of face. Russell *et al.* (1974) and Rochester and Topham (1979) have interpreted the IR spectra of goethite in terms of various types of surface OH groups (A, B, and C) that are present in different ratios in each type of face. The predominant and rather unreactive (100) face is relatively rich in B-type surface Fe ions strongly linked to the solid framework. It should be concluded that A-sites (singly coordinated OH groups) are involved in the interaction with D and L, although C (doubly coordinated) and B (triply coordinated) sites may also contribute.

There is a wide variety of models that describes the chemisorption of anions of different complexants onto metal oxides, that differs in the number of sites and coordination modes involved in the reaction: single site + single mode is the most simple, and shall be used whenever possible in the following discussion. Other models involve more than one adsorption mode onto a single type of site (e.g., dos Santos Afonso and Stumm, 1992) and multiple sites of various degrees of reactivity (e.g., the MUSIC model developed by Hiemstra *et al.*, 1989). For a detailed analysis of various models, see Blesa *et al.* (1992a). Two modes of EDTA adsorption on iron oxides are documented in the literature (Blesa *et al.*, 1984) and this result is used in our discussion.

Kinetics of dissolution. The role of surface complexes

The data in Figures 4–6 can be interpreted using the surface complexation approach by assuming that dissolution proceeds through the following steps: (a) competitive adsorption of dithionite D and EDTA or citrate L; (b) inner sphere redox decomposition of surface dithionite complexes, paralleling an outer sphere attack by dithionite on $\equiv Fe^{III}$-OH and $\equiv Fe^{III}$-L surface complexes; these reactions produce $\equiv Fe^{II}$ surface species; (c) phase transfer of $\equiv Fe^{II}$-OH and $\equiv Fe^{II}$-L to yield dissolved Fe^{II}-L complexes.

In the more general case, any of these processes may limit the overall rate. In practice, chemisorption of simple anions like $S_2O_4^{2-}$ or L^{n-} are known to be fast, and the corresponding formation reactions may be considered as equilibrated:

$$\equiv Fe^{III}\text{-OH} + D \overset{K_D(H^+)}{\rightleftharpoons} \equiv Fe^{III}\text{-D} \quad (3)$$

$$\equiv Fe^{III}\text{-OH} + L \overset{K_L(H^+)}{\rightleftharpoons} \equiv Fe^{III}\text{-L}. \quad (4)$$

https://doi.org/10.1346/CCMN.1992.0400512 Published online by Cambridge University Press

Eqs. (3) and (4) describe the adsorption of both reagents without addressing the problem of the detailed characterization of the surface species. Some information, including values of the constant K_L, is available for equilibrium (4) (Bowden *et al.*, 1980; Rueda *et al.*, 1985). Adsorption affinity is known to increase with decreasing pH, and more than one mode of adsorption is involved, corresponding to collapsed and extended configurations of EDTA on the surface (Blesa *et al.*, 1984). In the collapsed mode, the pairs of carboxylato groups at both ends of EDTA are bound to vicinal surface Fe centers, whereas in the extended configuration, the tail of the EDTA molecule points freely to the solution. At the EDTA concentrations used in this study, the latter mode prevails (Borghi *et al.*, 1989). EDTA adsorption reactions are known to be fast and reversible; for example, addition of Fe(III) to the solution produces the desorption by scavenging free EDTA anions from solution (Blesa *et al.*, 1984).

It is impossible to measure K_D [Eq. (3)] directly because of dissolution. The wealth of information on anion adsorption (Dzombak and Morel, 1990) suffices, however, to demonstrate that in this case affinity is expected to increase as the pH decreases. This pH dependence is the manifestation of the need to maintain low surface charges upon adsorption. The state of protonation of the adsorbed anions is not known, and it may change with pH. Eqs. (3) and (4) omit specifying the actual composition and charge of surface complexes. As K_D values are unknown, they were considered adjustable parameters in the fitting of the dissolution curves, as described below.

Dissolution of surface complexes

Goethite dissolves at a finite rate both in the absence and in the presence of very large excess of L. To account for dissolution in L-free media, Eq. (5) should be written:

$$\equiv Fe^{III}\text{-}D \xrightarrow{k_0} Fe^{II}_{aq} + \text{oxidation products of } S_2O_4^{2-} \quad (5)$$

$$R_1 = k_0\{\equiv Fe^{III}\text{-}D\}. \quad (6)$$

In order to account for the finite rate of dissolution observed at very high [L] values, it is necessary to postulate that $S_2O_4^{2-}$ may also attack ≡Fe-L surface complexes, probably *via* outer sphere electron transfer:

$$\equiv Fe^{III}\text{-}L + S_2O_4^{2-} \rightarrow Fe^{II} + \text{oxidation products of } S_2O_4^{2-} \quad (7)$$

$$R_3 = k_2[D]^n\{\equiv Fe^{III}\text{-}L\}. \quad (8)$$

The kinetic order n on $S_2O_4^{2-}$ is discussed below.

Synergistic effects

A simple kinetic scheme involving only R_1 and R_3 should lead, because of competition between L and D for surface centers, to a straight line in Figures 4 and 5, with all the rates ranging between R_1 and R_3. The maxima in Figures 4 and 5 require that cooperative effects be taken into account.

The simplest explanation of the influence of EDTA and citrate at constant dithionite concentration is that the co-adsorption of ligand and reductant onto vicinal sites promotes dissolution:

$$\left|\begin{matrix}\equiv Fe^{III}\text{-}OH \\ \equiv Fe^{III}\text{-}L\end{matrix}\right. + S_2O_4^{2-} \overset{K_D(H^+)}{\rightleftharpoons} \left|\begin{matrix}\equiv Fe^{III}\text{-}D \\ \equiv Fe^{III}\text{-}L\end{matrix}\right. \downarrow k_1$$

$$Fe^{II}_{aq} + \text{oxidation products of } S_2O_4^{2-} \quad (9)$$

$$R_2 = k_1\left\{\left|\begin{matrix}\equiv Fe\text{-}D \\ \equiv Fe\text{-}L\end{matrix}\right|\right\} \quad (10)$$

(the label that indicates the oxidation state of surface Fe has been deleted for simplicity).

There are several possible explanations for enhanced reactivity, i.e., $k_1 > k_0$ for such an ensemble. The simplest one is based on the conformation of EDTA: the carboxylato groups of the free end in the extended configuration are available for interaction with surface Fe-dithionite complexes, either before or immediately after redox decomposition. In the former case, a mixed ligand complex is formed on the surface. In the second case, the activation energy for dissolution may be lowered by the immediate availability of complexant. Related examples refer to dissolution by ascorbate (dos Santos Afonso *et al.*, 1990) and by EDTA/phosphate mixtures (Borggaard, 1991).

If $k_1 > k_0$, a rate enhancement ensues upon addition of L at low degrees of coverage. At higher concentrations of $S_2O_4^{2-}$ and/or L, the net influence depends on the actual value of the ratio k_1/k_0 and on the ratio $K_L[L]/K_D[D]$.

The overall rate of reaction is given by:

$$\begin{aligned} R &= R_1 + R_2 + R_3 \\ &= k_0\{\equiv Fe\text{-}D\} + k_1\{\equiv Fe_2\text{-}DL\} \\ &\quad + k_2[D]^n\{\equiv Fe\text{-}L\}. \end{aligned} \quad (11)$$

In Eq. (11) the surface complexes are identified by the number of surface Fe ions involved, and by the bound ligand (dithionite D and/or complexant L).

To write the overall rate in terms of the contribution of these three parallel paths, it is convenient to describe all these paths in terms of dimeric sites:

$\left\|\begin{matrix}\equiv Fe\text{-}OH \\ \equiv Fe\text{-}D\end{matrix}\right.$	$\left\|\begin{matrix}\equiv Fe\text{-}D \\ \equiv Fe\text{-}D\end{matrix}\right.$	$\left\|\begin{matrix}\equiv Fe\text{-}D \\ \equiv Fe\text{-}L\end{matrix}\right.$	$\left\|\begin{matrix}\equiv Fe\text{-}L \\ \equiv Fe\text{-}L\end{matrix}\right.$
I	II	III	IV

There are two further possible dimeric sites

$$\left|\begin{matrix}\equiv Fe\text{-}OH \\ \equiv Fe\text{-}OH\end{matrix}\right. \quad \text{and} \quad \left|\begin{matrix}\equiv Fe\text{-}OH \\ \equiv Fe\text{-}L\end{matrix}\right.$$

V VI

These two combinations are not included in the anal-

https://doi.org/10.1346/CCMN.1992.0400512 Published online by Cambridge University Press

Table 1. Parameters and measured constants used to fit experimental data by Eq. (12) (pH 7.3, T = 315 K).

Parameter	Value		Units	Comments
	L = EDTA	L = Cit		
K_L	300	110	$mol^{-1}\ dm^3$	Rueda *et al.* (1985) Bowden *et al.* (1980)
K_S	250	250	$mol^{-1}\ dm^3$	Eq. (15); position of the maxima in Figures 4 and 5
N_sk_o	1.75×10^{-3}	1.75×10^{-3}	s^{-1}	Eq. (15). Note that $R = \{df/dt\}_{t=0}$
N_sk_1	1.76×10^{-2}	10^{-2}	s^{-1}	Eq. (15). Note that $R = \{df/dt\}_{t=0}$
$N_sk_2^*$	7.6×10^{-4}	5×10^{-4}	s^{-1}	$k_2^* = k_2\,[D]^n$
n	0.35	0.5	—	Eq. (17)
n′	0.5	0.6	—	Eq. (24)

ysis because they are assumed not to contribute appreciably to the rate. V would be important only at low L concentrations, and under these conditions inner sphere pathways predominate. VI is not important in any of our experimental conditions: the speciation analysis described below illustrates this point.[1] The sites labeled as ≡Fe-OH (and probably ≡Fe-D and ≡Fe-L, as well) describe the whole suite of sites related by protolytic equilibria, e.g., $\equiv Fe\text{-}OH_2^+$, ≡Fe-OH and $\equiv FeO^-$.

The rate expression in terms of surface complexes I–IV is:

$$R = \frac{N_s}{2}(2k_0\theta_0\theta_1 + 2k_0\theta_1^2 + 2k_1\theta_1\theta_2 + 2k_2[D]^n\theta_2^2) \quad (12)$$

where it has been assumed that the reactivity of dimeric sites II and IV is twice that of the corresponding monomers; the factors of two appearing in the first two terms of (12) represent, respectively, the statistical probability factor of an ensemble of two dissimilar sites, I, and the enhanced probability of dissolution of II. In (12), θ_0, θ_1, and θ_2 are the degrees of coverage by OH^-, D, and L respectively, and N_s the total density of adsorption sites. For competitive adsorption,

$$\theta_0 = 1/\{1 + K_D[D] + K_L[L]\} \quad (13)$$

$$\theta_1 = K_D[D]/\{1 + K_D[D] + K_L[L]\} \quad (14)$$

$$\theta_2 = K_L[L]/\{1 + K_D[D] + K_L[L]\}. \quad (15)$$

These equations describe a simple version of the more general case analyzed by Wieland *et al.* (1988) through the use of lattice statistics. This formalism also assumes Langmuir-type isotherms, valid in its more restricted form only when the surface potential is zero. It has been repeatedly shown, however, that even when charge develops on the surface, the adsorption density is much larger than the charge density: only a minor fraction of adsorbed species bear a net charge. Consequently, anion adsorption can be described disregarding the correction introduced by the electrostatic term, by simply using a conditional equilibrium constant.

From (13)–(15) the rate is

$$R = \frac{N_s}{\{1 + K_D[D] + K_L[L]\}^2} \times \{k_0K_D[D] + k_0K_D^2[D]^2 + k_1K_DK_L[D][L] + k_2K_L^2[D]^n[L]^2\}. \quad (16)$$

Eq. (16) can be shown to be consistent with all possible limiting conditions. For example, for [L] = 0, it is equivalent to the simple Langmuir description assuming the formation of single ≡Fe-D sites.

At constant [D], R is a function of [L]. Under the conditions of Figures 4 and 5, it can be shown that R goes through a maximum when $K_L[L]$ is of the order of unity, provided that $k_1 > 4k_2[D]^n$. This relation is fulfilled in our system, as shown by the values reported below (see Table 1). The conditions of the maximum also correspond to the maximum of $\theta_1\theta_2$.

The parameters required to interpret the result are K_D and the composite magnitudes N_Sk_0, N_Sk_1 and $N_Sk_2^* = N_Sk_2[D]^n$. The values that best fit the kinetic data are shown in Table 1, together with the values used for K_L. The curves corresponding to Eq. (16) are shown with the experimental data in Figures 4 and 5. It may be seen that at pH 7.3, the affinities for EDTA and dithionite are similar; this finding is reasonable because at this pH value the adsorption affinity of EDTA is drastically lowered by the protonation requirement (Blesa *et al.*, 1984; Rueda *et al.*, 1985), whereas the affinity of dithionite is expected to be less sensitive to pH in this range.

The strong dependence of dissolution rates on [L] at very low [L] reflects the fast changes in the surface sites distribution (see Figures 10 and 11). The maximum in the rate of dissolution is coincident with the maximum in the fraction of mixed dimeric sites ($\theta_1\theta_2$). Because of the larger K_L value for EDTA than for citrate and the lower dithionite concentration, the maximum θ_{DL}

[1] The reactivity of VI towards outer-sphere attack by dithionite can, in principle, be assumed similar to that of IV; but VI may further react by inner-sphere mechanisms mediated by III. Operation of the outer-sphere pathway require dithionite concentrations high enough to enact the VI → III transformation.

https://doi.org/10.1346/CCMN.1992.0400512 Published online by Cambridge University Press

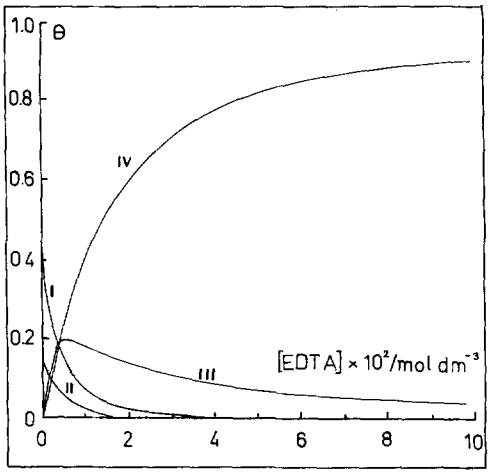

Figure 10. Surface sites distribution as a function of [EDTA]. $[S_2O_4^{2-}] = 2.55 \times 10^{-3}$ mol dm^{-3}; pH 7.3; T = 315 K. Species are identified by roman numerals as described in the text.

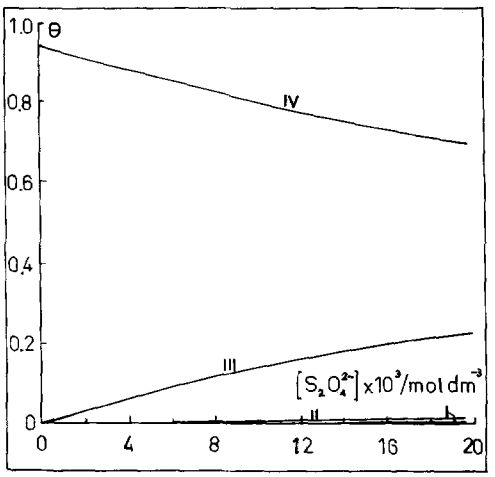

Figure 12. Surface sites distribution as a function of $[S_2O_4^{2-}]$. [EDTA] = 0.1 mol dm^{-3}; pH 7.3; T = 315 K. Species are identified by roman numerals as described in the text.

value is lower for EDTA and obtained at lower ligand concentration. However, the maximum rates themselves are similar because k_1 is larger for EDTA (see Table 1).

The outer sphere pathway

By measuring the dependence of the rate on [D] at constant and large concentration of L, the order n of the outer sphere process can, in principle, be evaluated: the rate expression (16) simplifies to

$$R = N_s k_2 [D]^n. \qquad (17)$$

This limiting condition is however not achieved in our experiments, and surface ≡Fe-D complexes are always present. Figure 12 shows the surface speciation in the presence of EDTA and of variable amounts of dithionite; the distribution in the case of citrate is similar. Under these conditions, the rate expression is still composed of two terms:

$$R = \frac{N_s}{\{1 + K_D[D] + K_L[L]\}^2} \times \{k_1 K_D K_L [D][L] + k_2 K_L^2 [L]^2 [D]^n\}. \qquad (18)$$

Calling $Q = R\{1 + K_D[D] + K_L[L]\}^2 - N_s k_1 K_D K_L [D][L]$, n can be derived graphically from the slope of a plot of log Q *vs* log [D]. From Figures 13 and 14, n is found to be 0.5 and 0.35 for citrate and EDTA, respectively. For the sake of simplicity, the above discussion of the mechanism of this pathway has been assumed to involve outer sphere redox reaction between dithionite and ≡Fe-L complexes. The values of n are in line with this assumption, and would represent the dependence on dithionite concentration of the formation of surface ion pairs (Davis *et al.*, 1978):

$$\equiv\text{Fe-L} + D = \equiv\text{Fe-L} \ldots D. \qquad (19)$$

In fact, the actual mechanism of reaction may be appreciably different; note that the charges omitted in Eq. (19) would make the pair ≡Fe-L . . . D very unstable. Two other mechanistic possibilities are: (a) Dithionite actually displaces L from the surface complexes, even at the highest L concentrations; this assumption leads to zero rates at [L] → ∞. (b) Outer sphere reaction rates are in fact controlled by the dissociation equilibrium of $S_2O_4^{2-}$ in solution, $SO_2^{\cdot-}$ being the actual reductant:

$$S_2O_4^{2-} \leftrightarrows 2\,SO_2^{\cdot-}; \qquad K_{20} \qquad (20)$$

$$\equiv\text{Fe-L} + SO_2^{\cdot-} = \equiv\text{Fe-L} \ldots SO_2^{\cdot-}; \qquad K_{21} \qquad (21)$$

$$\equiv\text{Fe-L} \ldots SO_2^{\cdot-} \xrightarrow{\text{slow}} Fe^{II}_{aq} + SO_2; \qquad k_{22}. \qquad (22)$$

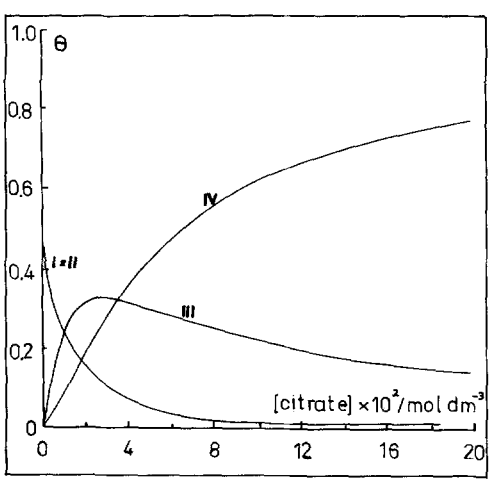

Figure 11. Surface sites distribution as a function of [citrate]. $[S_2O_4^{2-}] = 7.67 \times 10^{-3}$ mol dm^{-3}; pH 7.3; T = 315 K. Species are identified by roman numerals as described in the text.

https://doi.org/10.1346/CCMN.1992.0400512 Published online by Cambridge University Press

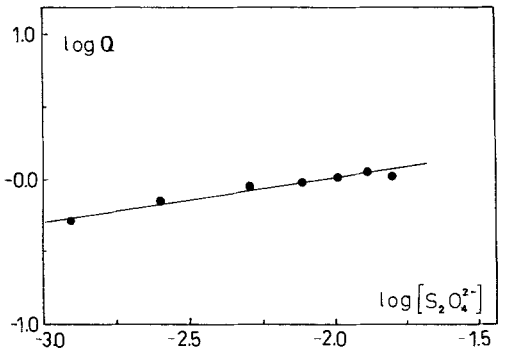

Figure 13. Doubly logarithmic plot of Eq. (17): log Q *vs* log[$S_2O_4^{2-}$]; [EDTA] = 0.1 mol dm^{-3}; T = 315 K; pH 7.3. For a definition of Q, see text. The slope is the reaction order on $S_2O_4^{2-}$ of the outer sphere pathway.

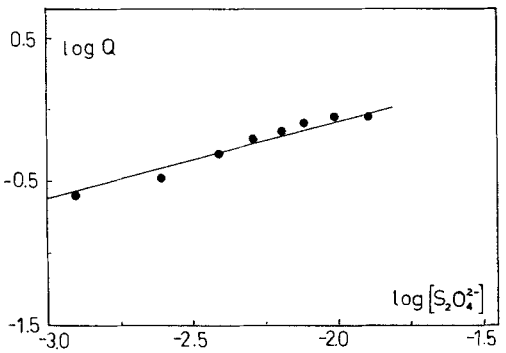

Figure 14. Doubly logarithmic plot of Eq. (17): log Q *vs* log[$S_2O_4^{2-}$]; [citrate] = 0.3 mol dm^{-3}; T = 315 K; pH 7.3. For a definition of Q, see text. The slope is the reaction order on $S_2O_4^{2-}$ of the outer sphere pathway.

This scheme leads to n = 0.5, as has been found for some homogeneous reactions of dithionite (Lambeth and Palmer, 1973; Balahura and Johnson, 1987). Furthermore, the lower negative charge of SO_2^- would make outer sphere adsorption of this ion more likely than that of $S_2O_4^{2-}$, but still with a low adsorption constant K_{21}.

$$\{\equiv\text{Fe-L} \ldots \text{SO}_2^-\} = K_{21}\{\equiv\text{Fe-L}\}[\text{SO}_2^-]$$
$$= K_{21}K_{20}^{1/2}\{\equiv\text{Fe-L}\}[S_2O_4^{2-}]^{-1/2} \quad (23)$$

This last possibility is most likely. Dissolution at very high [L] is an outer sphere process, mediated by the radical ions SO_2^- that are weakly adsorbed in the outer Helmholtz plane. The rate constant k_2 is thus interpreted as

$$k_2 = k_{22}K_{21}K_{20}^{1/2}. \quad (24)$$

The influence of pH

Figure 7 shows the dissolution rate as a function of pH. Although the reducing power of dithionite decreases upon lowering pH, the dissolution rate increases. This result shows clearly that the redox potential of dithionite is not an important parameter to define the dissolution rate. The data in Figure 7 fit Eq. (25):

$$R = k[H^+]^{n'} \quad (25)$$

where n' = 0.6 when the ligand is citrate and 0.5 when it is EDTA. These exponents are typical of dissolution kinetics (Blesa *et al.*, 1984, 1987, 1988; Hidalgo *et al.*, 1988) and evidence the importance of the protonation on the adsorption equilibria, generally described by a Freundlich isotherm. Eq. (25) represents a requirement for protons adjacent to the dissolution site (Blesa *et al.*, 1986; Valverde, 1976).

The pH dependency is not particularly revealing of possible mechanistic changes as the pH is lowered. In the experiments in more acidic media, dithionite is rapidly consumed by its decomposition. For example, it has been reported (Wayman and Lem, 1970) that at pH 4 and 296 K, dithionite concentration falls rapidly to zero after an induction period of around 5 min. The same autoacceleratory behavior has been reported at higher pH values, but with a longer time scale (e.g., 20 min at pH 6 and 333 K) (Rinker *et al.*, 1965).[2]

Depletion of the reductant does not arrest the dissolution reaction if enough Fe^{II} has been released in the presence of EDTA or citrate and the pH is low enough. In such a case, dissolution may proceed through the well-known reductive dissolution by ferrous carboxylate complexes (Blesa *et al.*, 1988), as described by Eq. (26), where X stands for OH or any other bound ligand.

$$\equiv Fe^{III}\text{-X} + L + Fe^{II}\text{-}L_{(aq)}$$
$$\rightarrow Fe^{II}\text{-}L_{(aq)} + Fe^{III}\text{-}L_{(aq)} + X \quad (26)$$

Torres *et al.* (1990) found a similar trend for the dissolution of hematite and magnetite by carboxylic acids and proposed the following kinetic law:

$$R = R_0 + kR_0t \quad (27)$$

where R_0 is the dissolution rate through the reductive action of carboxylate, R_0t represents the instantaneous Fe^{II} concentration, and k is the rate constant for the dissolution brought about by Fe^{II}-L complexes. Eq. (27) represents an autoacceleratory profile of [Fe] *vs* t, but the induction period may become blurred in the case of fast reactions.

These acidic media are not very convenient for analytical use of dithionite. The rate of decomposition is not only fast, but also subject to several possible catalytic effects, and it is difficult to control the extent of reductive dissolution by Fe^{II}-L. This latter process puts

[2] Dithionite decomposition has been reported to be oscillatory (De Poy and Mason, 1975); such a feature is not important in its use as a dissolution reagent, except for the fact that it illustrates the complexity of the involved chemistry.

https://doi.org/10.1346/CCMN.1992.0400512 Published online by Cambridge University Press

Fe^{III} and not Fe^{II} in solution, that is homogeneously reduced by the excess of dithionite (Borghi *et al.*, 1991).

Application to soil analysis

The dependence of the rate on temperature, shown in Figure 9 for the case of L = citrate, is typical of iron(III) oxides dissolution (Bruyère and Blesa, 1985; Segal and Williams, 1986; Hidalgo *et al.*, 1988). The advantages of using higher temperatures for faster soil analysis must be balanced by the increased rate of $S_2O_4^{2-}$ decomposition. We have found that temperatures of about 313 K seem to be adequate for soil analysis.

The application of these results to soil analysis suggests the convenience of working in more acidic media (pH 5.5), under N_2 and at lower temperature than in the traditional Mehra and Jackson procedure. Higher acidities should be avoided not only to prevent reagent decomposition, but also to avoid less selective dissolution. Repeated addition of dithionite is unnecessary if adequate control of these variables is maintained. In particular, it should be recognized that effective Fe extraction in slightly acidic or nearly neutral media requires the use of strong reductants such as dithionite or the recently proposed Ti(III) carboxylates (Ryan and Gschwend, 1991), which are not very stable in aqueous media. Adequate protection from air is therefore required for efficient use of the reductant, and temperature should not be indiscriminately raised.

ACKNOWLEDGMENTS

This work was supported by CONICET, CICPBA, Universidad Nacional del Sur and CNEA. M.A.B. is a member of CONICET. R.L.G. is a member of CICPBA.

The authors wish to thank Dr. Ryan (MIT) for his careful and detailed comments on the early version of the paper, which were instrumental in the preparation of the present version.

REFERENCES

Aguilera, N. H., and Jackson, K. L. (1953) Iron oxide removal from soils and clays: *Soil Sci. Soc. Amer. Proc.* **17**, 359–364.

Ardizzone, S., and Formaro, L. (1983) Temperature induced phase transformation of metastable $Fe(OH)_3$ in the presence of ferrous ions: *Materials Chem. Phys.* **8**, 125.

Atkinson, R. J., Posner, A. M., and Quirk, J. P. (1968) Crystal nucleation in Fe(III) solutions and hydroxide gels: *J. Inorg. Nucl. Chem.* **30**, 2371–2381.

Balahura, R. J., and Johnson, M. D. (1987) Outer-sphere dithionite reductions of metal complexes: *Inorg. Chem.* **26**, 3860.

Baumgartner, E., Blesa, M. A., Marinovich, H. A., and Maroto, A. J. G. (1983) Heterogeneous electron transfer as a pathway in the dissolution of magnetite in oxalic acid solutions: *Inorg. Chem.* **22**, 2224.

Blesa, M. A., and Maroto, A. J. G. (1986) Dissolution of metal oxides: *J. Chim. Phys.* **83**, 757–764.

Blesa, M. A., Regazzoni, A. E., and Maroto, A. J. G. (1988) Reactions of metal oxides with aqueous solutions: *Mater. Sci. Forum* **29**, 31–98.

Blesa, M. A., Regazzoni, A. E., and Morando, P. J. (1992a) *Chemical Dissolution of Metal Oxides:* CRC Press, Boca Raton, Florida, in press.

Blesa, M. A., Regazzoni, A. E., and Stumm, W. (1992b) *Surface Complexes as Reactive Species in Metal Oxide Dissolution,* unpublished.

Blesa, M. A., Borghi, E. B., Maroto, A. J. G., and Regazzoni, A. E. (1984) Adsorption of EDTA and iron-EDTA complexes on magnetite and the mechanism of dissolution of magnetite by EDTA: *J. Colloid Interface Sci.* **98**, 295–305.

Blesa, M. A., Marinovich, H. A., Baumgartner, E. C., and Maroto, A. J. G. (1987) Mechanism of dissolution of magnetite by oxalic acid-ferrous ion solutions: *Inorg. Chem.* **26**, 3713–3717.

Borggaard, O. K. (1991) Effects of phosphate on iron oxide dissolution in EDTA and oxalate: *Clays & Clay Minerals* **39**, 324–327.

Borghi, E. B., Morando, P. J., and Blesa, M. A. (1991) The dissolution of magnetite by mercaptocarboxylic acids: *Langmuir* **7**, 1652–1659.

Borghi, E. B., Regazzoni, A. E., Maroto, A. J. G., and Blesa, M. A. (1989) Reductive dissolution of magnetite by solutions containing EDTA and Fe(II): *J. Colloid Interface Sci.* **130**, 299–310.

Bowden, J. W., Nagarajah, N. J., Barrow, N. J., Posner, A. M., and Quirk, J. P. (1980) Describing the adsorption of phosphate, citrate, and selenite on a variable-charge mineral surface: *Aust. J. Soil Res.* **18**, 49–60.

Brown, W. E., Dollimore, D., and Galwey, A. K. (1980) *Reactions in the Solid State. Comprehensive Chemical Kinetics, Vol. 22,* C. H. Bamford and C. F. H. Tipper, eds., Elsevier, Amsterdam.

Bruyère, V. I. E., and Blesa, M. A. (1985) Acidic and reductive dissolution of magnetite in aqueous sulfuric acid: *J. Electroanal. Chem.* **182**, 141–156.

Cornell, R. M., Posner, A. M., and Quirk, J. P. (1974) Crystal morphology and the dissolution geothite: *J. Inorg. Nucl. Chem.* **36**, 1937.

Cornell, R. M., Posner, A. M., and Quirk, J. P. (1976) Kinetics and mechanism of the acid dissolution of goethite (α-FeOOH): *J. Inorg. Nucl. Chem.* **38**, 563–567.

Davis, A. D., James, R. O., and Leckie, J. O. (1978) Surface ionization and complexation at the oxide/water interface. I. Computation of electrical double layer properties in simple electrolytes: *J. Colloid Interface Sci.* **63**, 480.

Deb, V. C. (1950) The estimations of free iron oxide in soils and clays and their removal: *J. Soil Sci.* **1**, 212–220.

De Poy, P. E., and Mason, D. M. (1975) Periodicity in chemically reacting systems: Model of the kinetic of the decomposition of sodium dithionite: *Faraday Symp. Chem. Soc.* **9**, 47–54.

dos Santos Afonso, M., and Stumm, W. (1992) The Reductive Dissolution of Iron (III)(Hydr)oxides by Hydrogen Sulfide: to be published.

dos Santos Afonso, M., Morando, P. J., Blesa, M. A., Banwart, S., and Stumm, W. (1990) The reductive dissolution of iron oxides by ascorbate: *J. Colloid Interface Sci.* **138**, 74–82.

Dzombak, D. A., and Morel, F. M. M. (1990) *Surface Complexation Modelling. Hydrous Ferric Oxide:* Wiley, New York.

Gorichev, I. G., and Kipriyanov, N. A. (1981) Kinetics of the dissolution of oxide phases in acids: *Russian J. Phys. Chem.* **55**, 1558–1568.

Hidalgo, M. del V., Katz, N. E., Maroto, A. J. G., and Blesa, M. A. (1988) The dissolution of magnetite by nitrilotri-

acetatoferrate(II): *J. Chem. Soc. Faraday Trans. I* **84,** 9–18.

Hiemstra, T., de Wit, J. C. M., and van Riemsdijk, W. H. (1989) Multisite proton adsorption modelling at the solid/solution interface of (hydr)oxides: A new approach. II. Application to various important (hydr)oxides: *J. Colloid Interface Sci.* **133,** 105–117.

Hingston, F. J., Posner, A. M., and Quirk, J. P. (1972) Anion adsorption by goethite and gibbsite. I. The role of the proton in determining adsorption envelopes: *J. Soil Sci.* **23,** 177.

Hsu, P. H. (1967) Determination of iron with thiocyanate: *Soil Sci. Soc. Am. Proc.* **31,** 353–355.

James, R. O., Stiglich, P. J., and Healy, T. W. (1975) Analysis of models of adsorption of metal ions at oxide water interface: *Disc. Faraday Soc.* **59,** 142.

Lambeth, D. O., and Palmer, G. (1973) The kinetics and mechanism of reduction of electron transfer proteins and other compounds of biological interest by dithionite: *J. Biol. Chem.* **248,** 6095.

Litter, M. I., Baumgartner, E. C., Urrutia, G. A., and Blesa, M. A. (1991) Photodissolution of iron oxides III: The interplay of photochemical and thermal processes in maghemite/carboxylic acid systems: *Environmental Sci. Techn.* **25,** 1907–1913.

Mc Keague, J. A., and Day, J. H. (1966) Dithionite and oxalate-extractable Fe and Al as acids in differentiating various classes of soils: *Can. J. Soil Sci.* **46,** 13–22.

Mehra, O. P., and Jackson, M. L. (1960) Iron oxide removal from soils and clays by a dithionite-citrate system buffered with sodium bicarbonate: *Clays and Clay Minerals, Proc. 7th Natl. Conf.,* Ada Swineford, ed., Pergamon Press, New York, pp. 317–327.

Regazzoni, A. E., Urrutia, G. A., Blesa, M. A., and Maroto, A. J. G. (1981) Some observations on the composition and morphology of synthetic magnetites obtained by different routes: *J. Inorg. Nuc. Chem.* **43,** 1489–1493.

Rinker, R. G., Lynn, S., Mason, D. M., and Corcoran, W. H. (1965) Kinetics and mechanism of the thermal decomposition of sodium dithionite in aqueous solution: *Ind. Eng. Chem. Fund.* **4,** 282–288.

Rochester, C. H., and Topham, S. A. (1979) Infrared study of surface hydroxyl groups on goethite: *J. C. S. Faraday I* **75,** 591–602.

Rueda, E. H. (1988) Procesos de adsorción y disolución en la interfaz goetita/solución acuosa: Ph.D. thesis, Universidad Nacional del Sur (Bahía Blanca).

Rueda, E. H., Grassi, R. L., and Blesa, M. A. (1985) Adsorption and dissolution in the system goethite/aqueous EDTA: *J. Colloid Interface Sci.* **106,** 243–246.

Russell, J. D., Parfitt, R. L., Fraser, A. R., and Farmer, V. C. (1974) Surface structures of gibbsite, goethite, and phosphated goethite: *Nature* **248,** 220–221.

Ryan, J. N., and Gschwend, P. M. (1991) Extraction of iron oxides from sediments using reductive dissolution by titanium(III): *Clays and Clay Minerals,* **39,** 509–518.

Segal, M. G., and Williams, W. J. (1986) Kinetics of metal oxide dissolution: *J. Chem. Soc. Faraday Trans. I* **82,** 3245.

Tamaura, Y., Ito, K., and Katsura, T. (1983) Transformation of γ-FeO(OH) to Fe_3O_4 by adsorption of iron(II) ion on γ-FeO(OH): *J. Chem. Soc. Dalton Trans.* 189–194.

Torrent, J., Schwertmann, U., and Barron, V. (1987) The reductive dissolution of synthetic goethite and hematite in dithionite: *Clay Miner.* **22,** 329–337.

Torres, R., Blesa, M. A., and Matijevic, E. (1990) Interactions of metal hydrous oxides with chelating agents. IX. Reductive dissolution of hematite and magnetite by aminocarboxylic acids: *J. Colloid Interface Sci.* **134,** 475–485.

Tronc, E., Jolivet, J. P., and Massart, R. (1982) Defect spinel structure in iron oxide colloids: *Mat. Res. Bull.* **17,** 1365–1369.

Valverde, N. (1976) Investigations on the rate of dissolution of metal oxides in acidic solutions with additions of redox couples and complexing agents: *Ber. Bunsenges Physik. Chem.* **80,** 333–340.

Wayman, M., and Lem, W. J. (1970) Decomposition of aqueous dithionite. II. Reaction mechanism for the decomposition of aqueous sodium dithionite: *Can. J. Chem.* **48,** 782–787.

Wieland, E., Wehrli, B., and Stumm, W. (1988) The coordination chemistry of weathering: III. A generalization on the dissolution rates of minerals: *Geochim. Cosmochim. Acta* **52,** 1969–1981.

(Received 9 April 1992; accepted 24 September 1992; Ms. 2137)